Cloud-Clone Corp.

Cloud-Clone Cardiovascular Disease Related Products & Animal Models

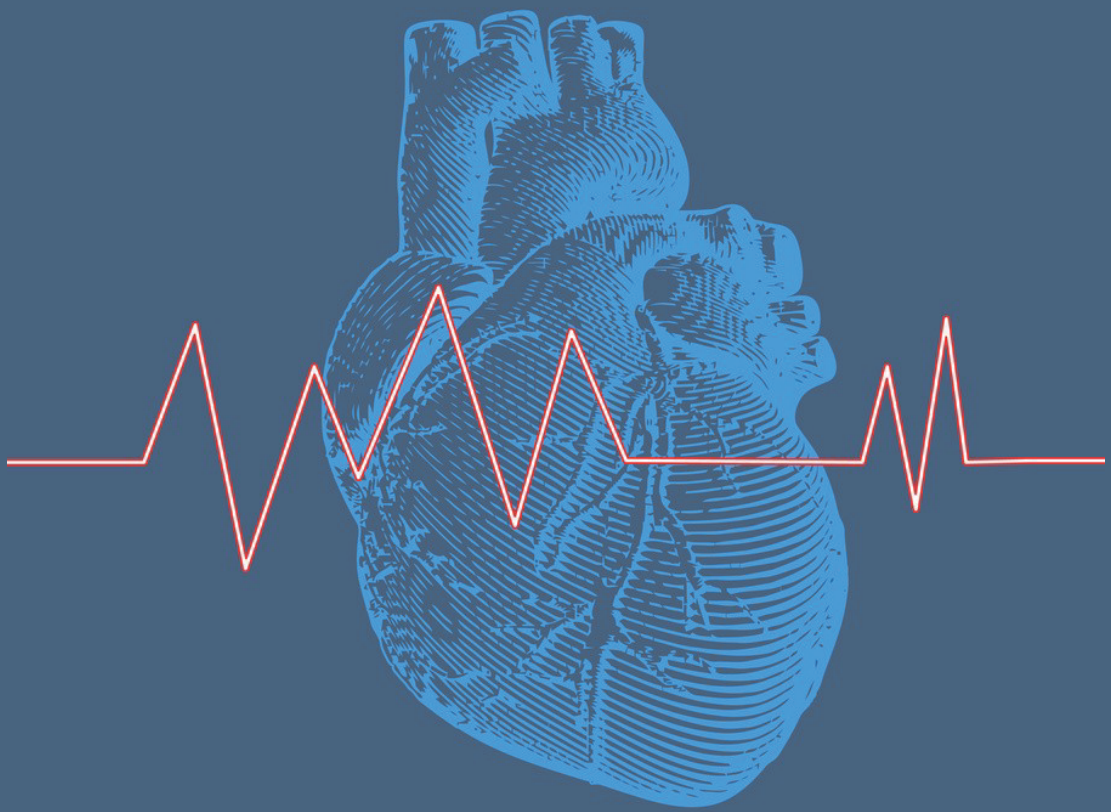

Cloud-Clone Corp.

Original manufacturer of assay reagent, analysis equipment and animal experiment service.

ISO 13485 ISO 9001

The cardiovascular system is composed of the heart and the vascular, which constitute the system for transporting blood. Cardiovascular activity can change cardiac output and peripheral resistance, coordinate blood flow distribution among organs and tissues under the mediation of nerve and body fluid, so as to meet the needs of blood flow in organs and tissues. The formation and development of heart and blood vessel, as well as the repair of injury and aging are regulated by many systems. Once these regulatory systems are confused, it will inevitably lead to metabolic disorders of heart and blood vessel cells, including the occurrence of cardiovascular diseases. According to current research, there are many cardiovascular-related signaling pathways, and the common pathways are roughly the following.

1.ENOS/NO signaling pathway: As a signal molecule, nitric oxide plays an important role in regulating blood pressure, maintaining vascular tension and regulating immune system in physiological activities. Abnormal NO is the cause of many cardiovascular diseases. Endothelial nitric oxide synthase, eNOS plays a major regulatory role as a rate-limiting enzyme in inducing NO synthesis.

2.Hippo-YAP signaling pathway: It plays a significant regulatory role in cell proliferation and apoptosis, and its core members include YAP and other proteins.

3.IL-33/ST2 signaling pathway: Soluble ST2 protein (sST2) is a member of the lL-1 receptor family, which can block the anti-cardiomyocyte hypertrophy and myocardial fibrosis effects of lL-33, leading to myocardial remodeling.

4.MTOR signaling pathway: mTOR kinase is a essential fator in regulating the homeostasis and growth of cardiomyocytes during development and postnatal period.

5.NOTCH signaling pathway: Notch signaling can be partly responsible for a variety of processes, such as angiogenesis, myogenesis, neurogenesis and hematopoiesis, and determine the growth, differentiation and survival of various cell types in different tissues.

2600+
Citations

181
Targets

Protein
Antibody
ELISA Kit

1. Excellent citations of Cardiovascular Biology related products(Excerpt)

Target	Species	Core No.	Journal	IF	Pubmed ID	Institute
AngII	Mouse	A005	European Heart Journal	23.425	26069213	Pharmakologisches Institut, Ruprecht-Karls-Universität Heidelberg
NT-ProBNP	Human	A485	European Heart Journal	23.425	24755006	Québec Heart & Lung Institute, Laval University
D2D	Human	A506	Circulation Research	15.211	28289017	Department of Cardiovascular Medicine, Tohoku University Graduate School of Medicine, Japan
MPO	Human	A601	Hepatology	14.079	27775820	Department of Molecular and Cellular Medicine, Institute of Liver and Biliary Sciences, New Delhi, India.
BK	Human	A874	Journal of Allergy and Clinical Immunology	13.258	29729940	Department of Emergency and Organ Transplantation, University "Aldo Moro"
ADAM10	Human	A766	Journal of Allergy and Clinical Immunology	13.258	22460069	Upper Airway Research Laboratory, Department of Otorhinolaryngology, Ghent University Hospital, Belgium.

CRP	Mouse	A821	Nature Communications	12.353	29410422	Cardiology and Angiology I, University Heart Center, and Medical Faculty, University of Freiburg
MMP1	Human	A097	European Heart Journal of heart failure	10.683	29709099	University of Navarra, CIMA, Program of Cardiovascular Diseases
LEP	Mouse	A084	PNAS	9.504	29784793	Peptide Biology Laboratories, Salk Institute, La Jolla
APOA1	Mouse	A519	Oncogene	6.854	26279300	Molecular and Cellular Biology Laboratory, Division of Basic Sciences, University of Crete Medical School

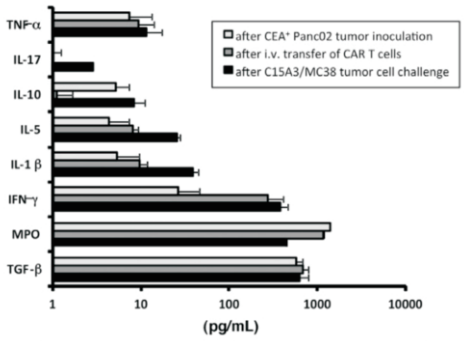

Figure . Secreted MPO and TGF-a were measured by enzyme-linked im-munosorbent assay (ELISA).(Markus Chmielewski, 2017)

(Product No.: SEA601Hu Sample type: cell line)

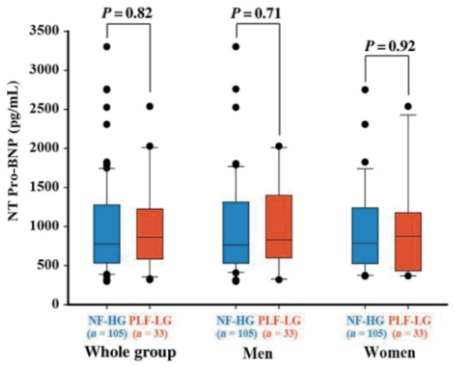

Figure . Comparison of NT pro-BNP between patients with paradoxical low-flow low gradient (PLF-LG), and normal-flow high gradient (NF-HG) in the whole Cohort A and in the subsets of men and women. (Marie-Annick Clavel, 2014)

(Product No.: SEA485Hu Sample type: plasma)

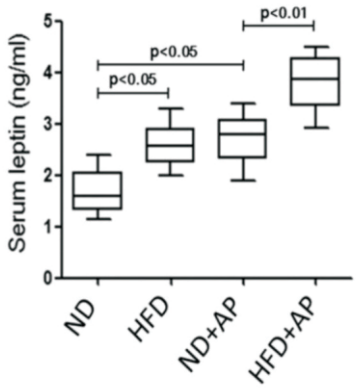

Figure . The serum levels of leptin (LEP) in rats were measured by ELISA. (Qian Wang, 2015)

(Product No.: SEA084Ra Sample type: serum)

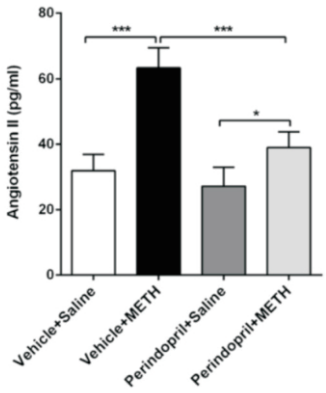

Figure . Ang II expression, as measured by ELISA, was down-regulated by perindopril in METH-treated mice. (Linhong Jiang, 2018)

(Product No.: SEA005Hu Sample type: cell line)

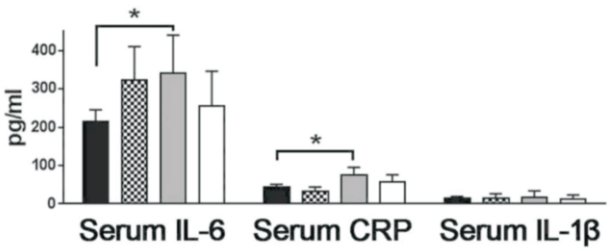

Figure . Serum levels of IL-6, CRP and IL-1β in the mice of 4 groups.(Cheng Ye, 2018)
(Product No.: SEA821Mu Sample type: serum)

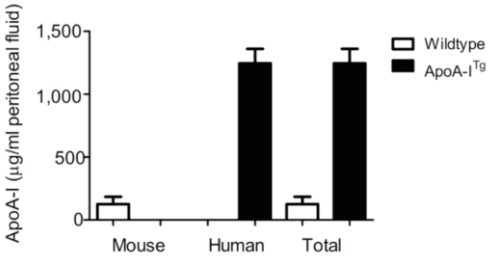

Figure . ApoA-I levels in mice and HDL modulated cytokine secretion after TLR activation. (Marjo M.P.C. Donners, 2016)
(Product No.: SEA519Mu Sample type: peritoneal fluid)

2. Citation statistics of Cardiovascular Biology related products (Excerpt)

Matrix Metalloproteinase 9 (MMP9)

Product	Species	Citation
Protein / Antibody / ELISA kit	Human, Rat, Mouse, Rabbit, Porcine, Bovine, Canine	128

Excerpt:

1. Li P, Sun Y, Liu Q. MicroRNA-340 induces apoptosis and inhibits metastasis of ovarian cancer cells by inactivation of NF-κB1[J]. Cellular Physiology and Biochemistry, 2016, 38(5): 1915-1927.（IF=5.5）
2. Bai Z, Wang J, Wang T, et al. The MiR-495/annexin A3/P53 axis inhibits the invasion and EMT of colorectal cancer cells[J]. Cellular Physiology and Biochemistry, 2017, 44(5): 1882-1895.（IF=5.5）
3. Corrado C, Saieva L, Raimondo S, et al. Chronic myelogenous leukaemia exosomes modulate bone marrow microenvironment through activation of epidermal growth factor receptor[J]. Journal of cellular and molecular medicine, 2016, 20(10): 1829-1839.
4. Yoshizaki K, Brito J M, Silva L F, et al. The effects of particulate matter on inflammation of respiratory system: Differences between male and female[J]. Science of the Total Environment, 2017, 586: 284-295.
5. Moustafa P E, Abdelkader N F, El Awdan S A, et al. Liraglutide ameliorated peripheral neuropathy in diabetic rats: Involvement of oxidative stress, inflammation and extracellular matrix remodeling[J]. Journal of neurochemistry, 2018.

C Reactive Protein (CRP)

Product	Species	Citation
Protein / Antibody / ELISA kit	Human, Rat, Mouse, Rabbit, Porcine, Bovine, Gallus	123

Excerpt:

1. Wolf D, Anto-Michel N, Blankenbach H, et al. A ligand-specific blockade of the integrin Mac-1 selectively targets pathologic inflammation while maintaining protective host-defense[J]. Nature communications, 2018, 9(1): 525.（IF=12.353）
2. Meng S. Resveratrol Inhibited Inflammation and Alveolar Bone Loss in Periodontitis[J]. Int J Dentistry Oral Sci. S, 2015, 6: 1-5.（IF=6.383）
3. Ye C, Wang R, Wang M, et al. Leptin alleviates intestinal mucosal barrier injury and inflammation in obese mice with acute pancreatitis[J]. International Journal of Obesity, 2018: 1.（IF=5.159）
4. Zhang L, Zhang T, Ding L, et al. The Protective Activities of Dietary Sea Cucumber Cerebrosides Against Atherosclerosis Through Regulating Inflammation and Cholesterol Metabolism in Male Mice[J]. Molecular nutrition & food research, 2018: 1800315.（IF=5.151）
5. Albert B B, De Bock M, Derraik J G B, et al. Among overweight middle-aged men, first-borns have lower insulin sensitivity than second-borns[J]. Scientific reports, 2014, 4: 3906.（IF=4.122）

Leptin (LEP)

Product	Species	Citation
Protein / Antibody / ELISA kit	Human, Rat, Mouse, Rabbit, Porcine, Canine, Gallus, Horse	118

Excerpt:

1. Yoon Y S, Tsai W W, Van de Velde S, et al. cAMP-inducible coactivator CRTC3 attenuates brown adipose tissue thermogenesis[J]. Proceedings of the National Academy of Sciences, 2018, 115(23): E5289-E5297.（IF=9.504）
2. Stygar D, Chełmecka E, Sawczyn T, et al. Changes of Plasma FABP4, CRP, Leptin, and Chemerin Levels in relation to Different Dietary Patterns and Duodenal-Jejunal Omega Switch Surgery in Sprague–Dawley Rats[J]. Oxidative medicine and cellular longevity, 2018, 2018.（IF=4.936）
3. Wu L, Bai Y, Liu M, et al. Transport mechanisms of butyrate modified nanoparticles: insight into “easy entry, hard transcytosis” of active targeting system in oral administration[J]. Molecular pharmaceutics, 2018, 15(9): 4273-4283.（IF=4.556）
4. Wang Q, Du J, Yu P, et al. Hepatic steatosis depresses alpha-1-antitrypsin levels in human and rat acute pancreatitis[J]. Scientific reports, 2015, 5: 17833.（IF=4.122）
5. Konieczna J, Sánchez J, Palou M, et al. Blood cell transcriptomic-based early biomarkers of adverse programming effects of gestational calorie restriction and their reversibility by leptin supplementation[J]. Scientific reports, 2015, 5: 9088.（IF=4.122）

Myeloperoxidase (MPO)

Product	Species	Citation
Protein / Antibody / ELISA kit	Human, Rat, Mouse, Rabbit, Porcine, Bovine, Gallus	105

Excerpt:

1. Chmielewski M, Hahn O, Rappl G, et al. T cells that target carcinoembryonic antigen eradicate orthotopic pancreatic carcinomas without inducing autoimmune colitis in mice[J]. Gastroenterology, 2012, 143(4): 1095-1107. e2.（IF=20.773）
2. Wang L, Zhang W, Ge C H, et al. Toll-like receptor 5 signaling restrains T-cell/natural killer T-cell activation and protects against concanavalin A–induced hepatic injury[J]. Hepatology, 2017, 65(6): 2059-2073.（IF=14.079）
3. Zhong R, Xie H, Kong F, et al. Enzyme catalysis–electrophoresis titration for multiplex enzymatic assay via moving reaction boundary chip[J]. Lab on a Chip, 2016, 16(18): 3538-3547.（IF=5.995）
4. Li M, Wang B, Sun X, et al. Upregulation of intestinal barrier function in mice with DSS-induced colitis by a defined bacterial consortium is associated with expansion of IL-17A producing gamma delta T cells[J]. Frontiers in immunology, 2017, 8: 824.（IF=5.511）
5. Wang B, Yang A, Zhao Z, et al. The Plasma Kallikrein–Kininogen Pathway is critical in the Pathogenesis of colitis in Mice[J]. Frontiers in Immunology, 2018, 9: 21.（IF=5.511）

Adiponectin (ADPN)

Product	Species	Citation
Protein / Antibody / ELISA kit	Human, Rat, Mouse, Rabbit, Porcine, Bovine, Gallus	105

Excerpt:

1. Hou N, Liu Y, Han F, et al. Irisin improves perivascular adipose tissue dysfunction via regulation of the heme oxygenase-1/adiponectin axis in diet-induced obese mice[J]. Journal of molecular and cellular cardiology, 2016, 99: 188-196.（IF=5.296）
2. Wolf D, Bukosza N, Engel D, et al. Inflammation, but not recruitment, of adipose tissue macrophages requires signalling through Mac-1 (CD11b/CD18) in diet-induced obesity (DIO)[J]. Thromb Haemost, 2017, 117(2): 325-38.（IF=4.952）
3. Chi Y, Li J, Li N, et al. FAM3A enhances adipogenesis of 3T3-L1 preadipocytes via activation of ATP-P2 receptor-Akt signaling pathway[J]. Oncotarget, 2017, 8(28): 45862.
4. Han F, Guo Y, Xu L, et al. Induction of haemeoxygenase-1 directly improves endothelial function in isolated aortas from obese rats through the Ampk-Pi3k/Akt-Enos pathway[J]. Cellular Physiology and Biochemistry, 2015, 36(4) 1480 1490

Angiotensin II (AngII)

Product	Species	Citation
Protein / Antibody / ELISA kit	Human, Rat, Mouse, Rabbit, Porcine, Bovine, Gallus	86

Excerpt:

1. Westermann D, Becher P M, Lindner D, et al. Biglcan is beneficial in angiotensin II induced heart failure by preventing cardiac inflammation and remodeling improving LV function and mortality by preventing transdifferentiation of myofibroblasts[J]. European Heart Journal, 2013, 34(suppl_1).（IF=23.425）
2. Camacho Londoño J E, Tian Q, Hammer K, et al. A background Ca2+ entry pathway mediated by TRPC1/TRPC4 is critical for development of pathological cardiac remodelling[J]. European heart journal, 2015, 36(33): 2257-2266.（IF=23.425）
3. Jiang L, Zhu R, Bu Q, et al. Brain Renin–Angiotensin System Blockade Attenuates Methamphetamine-Induced Hyperlocomotion and Neurotoxicity[J]. Neurotherapeutics, 2018: 1-11.（IF=5.719）
4. Motawi T K, Darwish H A, Hamed M A, et al. A therapeutic insight of niacin and coenzyme q10 against diabetic encephalopathy in rats[J]. Molecular neurobiology, 2017, 54(3): 1601-1611.（IF=5.076）

N-Terminal Pro-Brain Natriuretic Peptide (NT-ProBNP)

Product	Species	Citation
Protein / Antibody / ELISA kit	Human, Rat, Mouse, Rabbit, Porcine, Bovine, Gallus	68

Excerpt:

1. Clavel M A, Côté N, Mathieu P, et al. Paradoxical low-flow, low-gradient aortic stenosis despite preserved left ventricular ejection fraction: new insights from weights of operatively excised aortic valves[J]. European heart journal, 2014, 35(38): 2655-2662.（IF=23.425）
2. Belle V S, KRISHNANANDA PRABHU R V, Shetty R K, et al. N-Terminal-pro Brain Natriuretic Peptide in Assessing the Severity of Stable Coronary Artery Disease[J]. Journal of Clinical & Diagnostic Research, 2018, 12(8).（IF=6.217）
3. Bielecka-Dabrowa A, Sakowicz A, Misztal M, et al. Differences in biochemical and genetic biomarkers in patients with heart failure of various etiologies[J]. International journal of cardiology, 2016, 221: 1073-1080.
4. Lin Y H, Kuo C C, Lee C M, et al. 5-methoxytryptophan is a potential marker for post-myocardial infarction heart failure-a preliminary approach to clinical utility[J]. International journal of cardiology, 2016, 222: 895-900.

Oxidized Low Density Lipoprotein (OxLDL)

Product	Species	Citation
Protein / Antibody / ELISA kit	Human, Rat, Mouse, Porcine	68

Excerpt:

1. Niopek K, Üstünel B E, Seitz S, et al. A Hepatic GAbp-AMPK Axis Links Inflammatory Signaling to Systemic Vascular Damage[J]. Cell reports, 2017, 20(6): 1422-1434.（IF=8.032）
2. Douglas G, Bendall J K, Crabtree M J, et al. Endothelial-specific Nox2 overexpression increases vascular superoxide and macrophage recruitment in ApoE−/− mice[J]. Cardiovascular research, 2012, 94(1): 20-29.（IF=6.29）
3. Goo Y H, Son S H, Yechoor V K, et al. Transcriptional Profiling of Foam Cells Reveals Induction of Guanylate-Binding Proteins Following Western Diet Acceleration of Atherosclerosis in the Absence of Global Changes in Inflammation[J]. Journal of the American Heart Association, 2016, 5(4): e002663.

Nitric Oxide Synthase 2, Inducible (NOS2)

Product	Species	Citation
Protein / Antibody / ELISA kit	Human, Rat, Mouse, Rabbit, Porcine, Bovine, Gallus	66

Excerpt:

1. Diling C, Chaoqun Z, Jian Y, et al. immunomodulatory activities of a Fungal Protein extracted from Hericium erinaceus through regulating the gut Microbiota[J]. Frontiers in immunology, 2017, 8: 666.（IF=5.511）
2. Campo G M, Avenoso A, D'ascola A, et al. Adenosine A2A receptor activation and hyaluronan fragment inhibition reduce inflammation in mouse articular chondrocytes stimulated with interleukin-1β[J]. The FEBS journal, 2012, 279(12): 2120-2133.
3. Filip G A, Postescu I D, Bolfa P, et al. Inhibition of UVB-induced skin phototoxicity by a grape seed extract as modulator of nitrosative stress, ERK/NF-kB signaling pathway and apoptosis, in SKH-1 mice[J]. Food and chemical toxicology, 2013, 57: 296-306.
4. Shahmohammadi A, Rousta A M, Azadi M R, et al. Soy isoflavone genistein attenuates lipopolysaccharide-induced cognitive impairments in the rat via exerting anti-oxidative and anti-inflammatory effects[J]. Cytokine, 2018, 104: 151-159.

Brain Natriuretic Peptide (BNP)

Product	Species	Citation
Protein / Antibody / ELISA kit	Human, Rat, Mouse, Porcine	54

Excerpt:

1. Lu D, Wang K, Wang S, et al. Beneficial effects of renal denervation on cardiac angiogenesis in rats with prolonged pressure overload[J]. Acta Physiologica, 2017, 220(1): 47-57.（IF=5.93）
2. Wei J, Guo F, Zhang M, et al. Signature-oriented investigation of the efficacy of multicomponent drugs against heart failure[J]. The FASEB Journal, 2018: fj. 201800673RR.（IF=5.595）
3. Li L, Ni J, Li M, et al. Ginsenoside Rg3 micelles mitigate doxorubicin-induced cardiotoxicity and enhance its anticancer efficacy[J]. Drug delivery, 2017, 24(1): 1617-1630.
4. Kovacevic L, Wolfe-Christensen C, Lu H, et al. Why does adenotonsillectomy not correct enuresis in all children with sleep disordered breathing?[J]. The Journal of urology, 2014, 191(5): 1592-1596.

Heme Oxygenase 1 (HO1)

Product	Species	Citation
Protein / Antibody / ELISA kit	Human, Rat, Mouse, Porcine	36

Excerpt:

1. Olkowicz M, Jablonska P, Rogowski J, et al. Simultaneous accurate quantification of HO-1, CD39, and CD73 in human calcified aortic valves using multiple enzyme digestion–filter aided sample pretreatment (MED-FASP) method and targeted proteomics[J]. Talanta, 2018, 182: 492-499.
2. Bae E H, Konvalinka A, Fang F, et al. Characterization of the intrarenal renin-angiotensin system in experimental alport syndrome[J]. The American Journal of Pathology, 2015, 185(5): 1423-1435.
3. Kabel A M, Atef A, Estfanous R S. Ameliorative potential of sitagliptin and/or resveratrol on experimentally-induced clear cell renal cell carcinoma[J]. Biomedicine & Pharmacotherapy, 2018, 97: 667-674.

3. Cloud-Clone Cardiovascular Biology related targets

Cloud-Clone Cardiovascular Biology related targets									
Target	Core No.	Target	Core No.	Target	Core No.	Target	Core No.	Target	Core No.
ACE	A004	APOM	C299	EDN2	F415	LOX1	B859	PRCP	B253
ACE2	B886	ARPC2	J601	EGF	A560	Lpa	A842	PROC	A734
ACTC1	B341	ARPC4	J599	EMILIN1	A415	MEF2A	C647	PTGDS	B640
ADAM10	A766	BCOR	C327	ES	A542	MMP1	A097	PTGIS	A740
ADMA	B301	BK	A874	ESM1	C463	MMP10	A098	REN	A889
ADP	A605	BMP10	C106	FABP2	A559	MMP14	C056	RETN	A847
ADRa1A	B298	BNP	A541	FABP3	B243	MMP23A	A211	S17aH	C016
ADRP	B350	CACT	B657	FABP4	B693	MMP25	B927	SALa	B892
AGE	B353	CALML3	F898	FATP5	B660	MMP3	A101	SALb	C026
AGER	A645	CALML5	F897	FCN2	B907	MMP8	A103	SOD1	B960
AGT	A797	CBFb	C361	FUM	B931	MMP9	A553	SOD2	B083
AGTR1	B658	CBY1	C364	gABA	A900	MPO	A601	TAZ	E564
aHSP	A412	CC16	A857	GAPDH	B932	MR	A464	TF	A524
ALOX5	B355	CDHH	B902	GATA4	A374	MSE	B433	TFPI2	B940
AngI	A811	ChAT	B929	GLP1	A804	MYH7B	P164	TIMP1	A552
AngII	A005	CKB	C030	GLUT4	C023	MYL1	B105	TIMP3	A129
AngIII	C312	CKM	A109	GP6	B904	MYL2	B102	TIMP4	A130
ANGPT1	A008	CKMT1A	A263	HAND1	C519	MYLK	B106	TM	A529
ANGPT2	A009	CLCF1	C389	HDL	B006	MYO	A480	TMOD1	G689
ANGPT4	A668	CNP	A721	HIF1a	A798	MYOG	B109	TMOD3	G687
ANGPTL2	B919	cPLA2	B624	HIF2a	D466	MYPN	G685	TNNC1	D227
ANGPTL4	B019	CRH	A835	HO1	A584	NMU	B025	TNNC2	D228
ANGPTL7	R176	CRIP1	C402	HOP	C532	NOS2	A837	TNNI1	D229
ANP	A225	CRP	A821	HSD11b1	C268	NOS3	A868	TNNI2	D230
APOA1	A519	CSE	B538	IDE	B897	NOSTRIN	A628	TNNI3	A478
APOA2	A604	CT1	A810	IGF1R	B659	NPR3	D046	TNNT1	D231
APOA4	B967	CX37	B466	IGFBP1	A052	NPY	A879	TNNT2	D232
APOA5	B997	CX40	B465	IMA	A825	NT-ProANP	A484	TNNT3	D233
APOB	C003	CX43	A277	ITLN1	A933	NT-ProBNP	A485	TWF1	M410
APOB100	A603	D2D	A506	LCN1	B706	OB	C039	VASN	G905
APOC2	B996	DA	A851	LDHA	B370	OxLDL	A527	VEGFB	A144
APOC3	B890	DDAVP	B841	LDHB	B698	PDK4	A958	VF	A638
APOC4	B828	DPP4	A884	LDLR	B008	PKCe	A439	VLDLR	B009
APOD	B968	DRD1	B299	LEP	A084	PKN2	B987		
APOE	A704	DSP	C203	LEPR	A083	PLA1	B151		
APOF	B879	ECE1	A483	LIPC	A769	PLN	B884		
APOH	A310	EDN1	A482	LIPD	A386	PPARg	A886		

4. Cloud-Clone Cardiovascular Disease Related Animal Models

Rat Model for Myocardial Infarction (MI) • DSI504Ra02

1. Anesthesia with 3% pentobarbital sodium at 30mg/kg by intraperitoneal injection, shave the chest and armpit hair with a shaving razor, expose the operation area and disinfect with iodine and 75% ethanol.

2. After anesthesia, the toe of the test can be performed without reaction. Open the external light microscope, open the ventilator, setting the parameters (respiratory ratio 2:1,Tidal volume 6~8ml,respiration frequency 75bpm). Tracheal intubation was inserted into the trachea along the glottis, and the rats were connected to the ventilator. The respiratory status of the mice was observed, and the chest beat was consistent with the frequency of the ventilator. The results indicated that the MI could be performed successfully.

3. The rats were placed in the right lateral recumbency position. Ophthalmic scissors were used to cut three or four intercostal chests under the armpit of the left forelimb. The heart was fully exposed with micro scissors, and a small amount of pericardium was gently clipped to expose the left anterior descending coronary artery (LAD).

4. Find the LAD direction or possible location under the microscope. A 5-0 suture with needle was taken from the needle holder, and the suture was passed through the left anterior descending coronary artery (LAD) next to the pulmonary artery below the root of the left atrial appendage to block the blood flow of the LAD.

5. The thoracic opening was sutured, the thoracic cavity was closed, and each layer of muscle and skin was sutured from the inside to the outside.

6. Pay close attention to the state of the mice after operation, whether there is abnormal breathing. After the mice were naturally recovered, the rats were removed from the ventilator and the trachea was removed.

Modeling Result

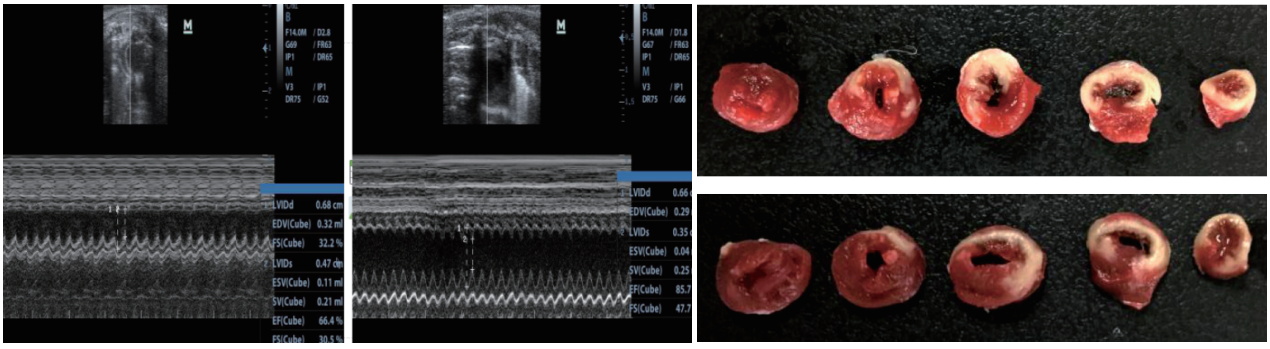

Fig. Ultrasonography images for rat heart of MI model (left); The TTC staining of rat heart of MI Model (right)

Mouse Model for Cardiac Hypertrophy (CH) • DSI548Mu03

1. Healthy male mice aged 6-8 weeks were selected as experimental subjects for SPF mice.
2. The weight of the mice was accurately weighed (g), and the mice were anesthetized by intraperitoneal injection. After the mice were fully anesthetized (about 3-5 minutes), the hair on the neck and chest of the mice was shaved with a mouse hair shaver (fully exposing the surgical area).
3. The mouse was inverted so that the mouse head was on the operator's side, and the head was raised. The middle of the neck was opened vertically to the beginning of the upper thoracic rib, and a 0.5mm incision was made down the midline of the rib at the beginning of the rib to expand the field of view, and the trachea from the neck was bluntly separated to the thymus. The aortic arch could be clearly seen by gently poking the free fat of the thymus. A 7-0 nonabsorbable suture was drawn from the base of the aortic arch, together with a homemade constriction tool (27G), to tighten the knot and withdraw the constriction tool. After completing the TAC operation, the mouse body temperature was maintained at around 37°C throughout the experiment.
4. The anterior opening of the chest cavity was sutured, and the skin incision was sutured completely with 5-0 sutures.
5. Pay close attention to the mouse status. After the mice woke up naturally, they were placed in a clean cage, filled in the operation record card, and returned to the rearing room to record the postoperative status and death of the mice.

Modeling Result

Fig. Picture of hearts

Cloud-Clone Corp.
Original Manufacturer for Assay Reagents, Testing Services and Diagnostic Reagents
23603 W. Fernhurst Dr., Unit 2201, Katy, TX 77494, USA Tel: 001-832-538-0970 Toll free: 888-960-7402 (In the USA)
www.cloud-clone.com www.cloud-clone.us